Photogrammetrie • Fernerkundung • Geoinformation 6/2005, S. 497–510, 6 figs., 2 tabs.

Land Deformation Measurement using SAR Interferometry: State-of-the-Art*

MICHELE CROSETTO, Barcelona, BRUNO CRIPPA, Milano, ERLINDA BIESCAS, ORIOL MONSERRAT, MARTA AGUDO, Barcelona & PAZ FERNANDEZ, Granada

Keywords: remote sensing, satellite, detection, modeling, software

Abstract: In the last fifteen years the differential interferometric SAR, Synthetic Aperture Radar, (DInSAR) techniques have demonstrated their potential as land deformation measurement tools. In the last few years their capability has been considerably improved by using large stacks of SAR images acquired over the same area, instead of the classical two images used in the standard configurations. With these advances the DInSAR techniques are becoming more and more quantitative geodetic tools for deformation monitoring, rather than simple qualitative tools. The goal of the paper is to review the state-of-the-art of the spaceborne DInSAR-based land deformation monitoring. The airborne DInSAR is not considered in this work. The paper begins with a concise description of some basic DInSAR concepts, followed by a discussion of the most important DInSAR applications. Then the state-of-the-art of DInSAR is analysed, by discussing few important technical issues, by addressing the issues of data and software availability, and by describing some relevant DInSAR results.

Zusammenfassung: *Stand der Bestimmung von Oberflächendeformationen mit SAR Interferometrie*. In den letzten fünfzehn Jahren haben die Techniken der differentiellen SAR Interferometrie (DInSAR) ihr Potenzial zur Bestimmung von Oberflächendeformationen gezeigt. In den letzten Jahren haben sich die Möglichkeiten durch die Verwendung einer großer Anzahl von SAR Bildern, die dasselbe Gebiet zeigen, im Gegensatz zu der klassischen Methode, die mit zwei Bildern arbeitet, deutlich verbessert. Durch diese Entwicklungen wird DInSAR zunehmend zu einem geodätischen Werkzeug zur quantitativen, und nicht nur zur qualitativen Deformationsbestimmung. Das Ziel dieses Beitrags ist es, den Stand von DInSAR in Wissenschaft und Technik für die Deformation der Landoberfläche mit weltraumgetragenen Sensoren zu beschreiben. Flugzeuggetragene Sensoren werden in diesem Artikel nicht berücksichtigt. Der Beitrag beginnt mit einer kurzen Beschreibung der Prinzipien von DInSAR, gefolgt von einer Vorstellung der wichtigsten DInSAR Anwendungen. Danach wird der Stand anhand einiger wichtiger technischer Aspekte sowie der Frage der Verfügbarkeit von Daten und Software und durch die Beschreibung einiger relevanter Ergebnisse diskutiert.

* Enhanced version of a paper published in the proceedings of the ISPRS Hannover Workshop 2005 "High Resolution Earth Imaging for Geospatial Information", May 17–20, 2005, Institute of Photogrammetry and GeoInformation, University of Hannover.

1432-8364/05/2005/0497 $ 3.50

1 Introduction

This paper is focused on the land deformation measurement based on the differential interferometric Synthetic Aperture Radar techniques (DInSAR). Its goal is to review the state-of-the-art of the DInSAR techniques that make use of data acquired by spaceborne SAR sensors. The airborne DInSAR, which still plays a minor role in deformation applications, is not considered in this work.

The DInSAR techniques exploit the information contained in the radar phase of at least two complex SAR images acquired in different epochs over the same area, and forming an interferometric pair. Unlike a simple amplitude SAR image, which only contains the amplitude of the SAR signal, a complex SAR image contains two components per pixel, from which the amplitude and phase signal can be derived. The phase is the key observable of all interferometric SAR techniques. The repeated acquisition of images over a given area is usually performed by using the same sensor, e. g. the Envisat ASAR, or sensors with identical system characteristics, as it was the case of ERS-1 and ERS-2. Only in particular cases it is possible to make cross-interferometry by using images acquired with different systems. One example, which is discussed later in this paper, is given by ERS and Envisat ASAR, e. g. see Arnaud et al. (2003). Besides the compatibility of the systems used for the repeat pass DInSAR, the condition of forming interferometric pairs imposes a severe constraint on the acquisition geometry. In order to obtain coherent SAR image pairs, i. e. couples of SAR images whose interferometric phase is useful for digital elevation model (DEM) generation (using interferometric SAR, InSAR, techniques) or deformation monitoring, the images have to share almost the same image geometry. In fact, the image acquisition from different viewpoints in space engenders a loss of coherence, which is called geometric decorrelation (Gatelli et al. 1994). For each SAR system there is a critical perpendicular baseline (the component of the vector that connects the two satellite positions during image acquisition, measured in the direction perpendicular to the SAR line-of-sight) which corresponds to a complete decorrelation of the interferometric phase. For instance, for ERS the critical baseline is about 1100 m: the employed baseline lengths are usually shorter, say of some hundreds of metres. An exception, as discussed in section 4, occurs using the so-called Persistent or Permanent Scatterers techniques that can exploit image pairs with baselines in the interval ± 1200 m (Colesanti et al. 2003a). This is due to the fact that the Persistent Scatterers that are smaller than the resolution cell have good coherence even for interferograms with baselines larger than the critical baseline. Anyways, the constraint on the baseline plays a key role for all DInSAR applications.

In the following, the principle of the DInSAR technique is briefly summarized. A scheme of the image acquisition is shown in Fig. 1, considering a single pixel footprint P:

– The sensor acquires a first SAR image at the time t_0, measuring the phase Φ_M. The

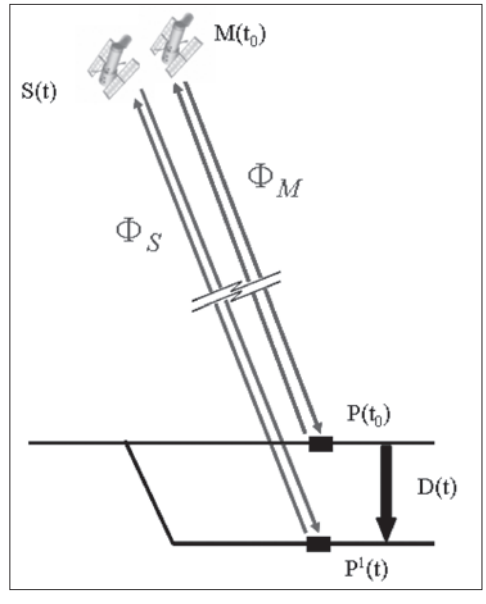

Fig. 1: Principle of DInSAR for deformation measurement.

first satellite and the corresponding image are usually referred as the master, M.
- Assuming that a land deformation D(t) occurs, which has a given evolution in time, the point P moves to P^1.
- The sensor acquires a second image at the time t, measuring the phase Φ_S. The second satellite is usually referred as the slave, S.

The InSAR techniques exploit the phase difference $\Phi_S - \Phi_M$, named interferometric phase $\Delta\Phi_{Int}$. Assuming that D(t) is naught, i. e. the terrain is stable and P^1 coincides with P, this phase is related to the distance difference $SP - MP$, which is the key element for the InSAR DEM generation. When the point moves from P to P^1 between two image acquisitions, besides the topographic phase component Φ_{Topo}, $\Delta\Phi_{Int}$ includes the terrain movement contribution, Φ_{Mov}:

$$\begin{aligned}\Delta\Phi_{Int} &= \Phi_S - \Phi_M \\ &= \frac{SP - MP}{\frac{\lambda}{4\cdot\pi}} + \frac{SP^1 - SP}{\frac{\lambda}{4\cdot\pi}} + \Phi_{Atm} + \Phi_{Noise} \\ &= \Phi_{Topo} + \Phi_{Mov} + \Phi_{Atm} + \Phi_{Noise}\end{aligned}$$

where Φ_{Atm} is the atmospheric contribution; Φ_{Noise} is the phase noise; SP^1 is the slave-to-P^1 distance; and λ is the radar wavelength. As mentioned above, by using the topographic component Φ_{Topo} it is possible to generate a DEM of the observed scene. In the DInSAR techniques the inverse transformation is used: if a DEM of the imaged scene is available, Φ_{Topo} is simulated and subtracted from $\Delta\Phi_{Int}$, obtaining the so-called DInSAR phase $\Delta\Phi_{D-Int}$:

$$\begin{aligned}\Delta\Phi_{D-Int} &= \Delta\Phi_{Int} - \Phi_{Topo\_Sim} = \\ &= \Phi_{Mov} + \Phi_{Atm} + \Phi_{\mathrm{Res}\_Topo} + \Phi_{Noise} \quad (1)\end{aligned}$$

where Φ_{Topo_Sim} is the simulated topographic component, and Φ_{Res_Topo} is the residual component due to errors in the simulation of Φ_{Topo}, e. g. due to errors in the employed DEM. In order to derive information on the terrain movement, Φ_{Mov} has to be separated from the other phase components. The techniques that use an external DEM in order to derive the topographic phase component use the so-called two-pass DInSAR configuration. There is another configuration, the three-pass one, which can work without an a priori known DEM, but which requires at least three images over the same scene (Zebker et al. 1994). For a general review of SAR interferometry, see Rosen et al. (2000) and Bamler & Hartl (1998).

In the following section some of the most important DInSAR applications are discussed. In the remaining part of the paper the state-of-the-art is analysed, by discussing the following topics:

- the number of SAR images used in the DInSAR procedures.
- the criteria used to select the pixels suitable to estimate the land deformation,
- the availability of DInSAR software tools,
- the available DInSAR satellite data,
- the quality and validation of the results.

2 DInSAR applications

Since the first description of the technique, which was based on L-band SEASAT SAR data (Gabriel et al. 1989), the great potential of DInSAR for land deformation applications has been recognized. Of major interest were, in particular, some typical features of the remote sensing systems, like the wide areas covered by the images, the global coverage and the repeat observation capabilities, associated with the intrinsic high metric quality of the DInSAR observations. In fact, since the beginning, it was clear that the spaceborne DInSAR is able to measure small deformations with high sensitivity, which is comparable to a small fraction of the radar wavelengths that are in the order of centimetres to few tens of centimetres. Later on, other important characteristics were recognized. Firstly, the high spatial resolution capability of the SAR systems, which in particular cases allows the deformation monitoring of small features, like buildings or infrastructures, to be per-

formed. Secondly, in the last years another aspect has gained importance: the availability of historical SAR datasets, which in the case of ERS1/2 covers almost 14 years.

In the last fifteen years many deformation-related DInSAR applications have been developed, and the capability of the D-InSAR techniques has been extensively documented. Hundreds of high level journal papers devoted to DInSAR have been published. A great contribution to this success certainly comes from the spectacular results achieved in different fields of geosciences. Some of the most relevant DInSAR application fields are listed below.

Seismology probably represents the field where the major number of scientific achievements have been obtained, including different types of coseismic studies, see e. g. Massonnet et al. (1993); postseismic deformation studies (Peltzer et al. 1996); and the monitoring of aseismic events (Rosen et al. 1998). It is worth emphasising that some of the above applications are characterized by very small deformations, e. g. less than 1 mm/yr for some aseismic and interseismic events. As it is described later in this paper, such deformations can only be achieved by using advanced DInSAR processing and analysis tools.

Vulcanology is another relevant application field, with several studies of volcanic deflation and uplift, e. g. see Amelung et al. (2000). Several examples of DInSAR applications to vulcanology are described in Massonnet & Sigmundsson (2000).
Different researches have been conducted in the field of glaciology, mainly on the ice sheets of Greenland and Antarctica. They included InSAR ice topography measurements (Kwok & Fahnestock 1996), ice velocity measurements (Goldstein et al. 1993), and other glaciological applications.

Landslides is another important application, where less results have been achieved so far, mainly due to the loss of coherence that usually characterises the landslides areas. However, with the Persistent Scatterers techniques for some types of landslide phenomena it seems to be possible to perform deformation measurements, e. g. see Colesanti et al. (2003b), and Hilley et al. (2004).

Ground subsidences and uplifts due to fluid pumping, construction works, geothermal activity, etc. have been described in several papers, see e. g. Amelung et al. (1999); Crosetto et al. (2003). Most of the published results concern urban areas, over which DInSAR data remains coherent over large observation periods. With the advent of the Persistent Scatterers techniques it is expected to get more and more deformation monitoring results outside the urban, suburban and industrial areas.

Finally, comprehensive reviews of different DInSAR geophysical applications are provided by Massonnet & Feigl (1998) and Hanssen (2001). An interesting link, where the latest DInSAR results based on data acquired by the ERS and Envisat satellites are described, is given by eopi.esa.int/esa/esa.

3 DInSAR and advanced DInSAR techniques

A large part of the DInSAR results mentioned above have been achieved by using the standard DInSAR configuration, i. e. by analysing a single differential interferogram derived from a pair of SAR images. This is the simplest DInSAR configuration, which often is the only one that can be implemented, due to the limited SAR data availability. However, as it is discussed later, the standard two-image configuration suffers important limitations. Even if for some types of application it may provide valuable results, e. g. for the estimation of large, say from decimetres to meters, deformation patterns, in general it is necessary to be aware of its limitations. A remarkable improvement in the quality of the DInSAR results is given by the new DInSAR methods that make use of large sets of SAR images acquired over the same deformation phenomenon. These techniques, hereafter called Advanced DInSAR (A-DInSAR) techniques, represent an outstanding advance with respect to the standard ones, both in terms of deformation modelling capabilities and quality of the deformation estimations.

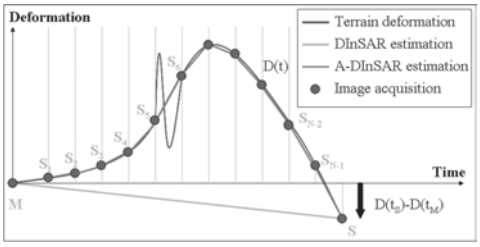

Fig. 2: Temporal sampling of a deformation phenomenon performed with the DInSAR and A-DInSAR techniques.

Temporal deformation modeling. As it is illustrated in Fig. 2, a standard DInSAR technique, which samples temporally a given deformation phenomenon with only two samples, a master image M and a slave one S, is only able to estimate the integrated deformation:

$$D_I(\Delta T) = D(t_S) - D(t_M),$$

or, equivalently, the linear deformation velocity between t_M and t_S. In contrast, the A-DInSAR techniques are in principle able of providing a whole description of the temporal behaviour of the deformation field at hand. This capability is clearly limited by the number N and the temporal distribution of the available SAR images. For instance, the highly non linear deformation that occurs between the acquisitions S_5 and S_6 in the example of Fig. 2 cannot be measured with the available SAR image acquisitions.

Quantitative vs. qualitative DInSAR. There is a second fundamental difference between DInSAR and A-DInSAR techniques. The standard configuration represents a zero-redundancy case, where it is not possible to check the presence of the different error sources that may affect the interferometric observations, or, equivalently, it is impossible to separate the movement component from the other phase components, see formula 1. For this reason the estimations derived with this configuration have, in general, a qualitative character and have to be employed with care. Note that in different applications some external information on the deformation under analysis may be available (e. g. a priori knowledge of stable areas, of the shape of the deformation field, etc.), which can considerably help in interpreting the DInSAR results. In contrast, the A-DInSAR methods may implement suitable data modelling and analysis procedures that associated with appropriate statistical treatments of the available DInSAR observations make possible the estimation of different parameters. The main parameters estimated by the DInSAR are briefly discussed below. In addition to this extended capability, the A-DInSAR techniques take usually advantage of a high data redundancy, which allows quantitative DInSAR results to be achieved, both in terms of precision and reliability.

1) By proper modelling the phase component due to terrain movement Φ_{Mov}, it is possible to estimate the spatial and temporal evolution of the deformation. The modelling strategies are strictly dependent on the type of application at hand. Anyway, the ability to fully describe a deformation phenomenon depends temporally on the number of available images, and spatially on the availability of "good pixels", i. e. pixels which are characterized by a low level of phase noise, Φ_{Noise}. This aspect is discussed in the following section. Often the temporal evolution of the deformation is modelled with linear functions, e. g. see (Ferretti et al. 2000, Ferretti et al. 2001). Crosetto et al. (2005) model the deformation by stepwise linear functions, whose parameters are computed by least squares adjustment. Other approaches allow a more complex description of the temporal behaviour of the deformation, see e. g. Lanari et al. (2004).

The complete estimation of the temporal evolution of deformation represents a remarkable improvement of the A-DInSAR techniques with respect to the standard DInSAR results. Fig. 3 shows an example which concerns the roof of an industrial building located in the metropolitan area of Barcelona. This result was obtained in the frame of an ESA funded Project named "Develop-

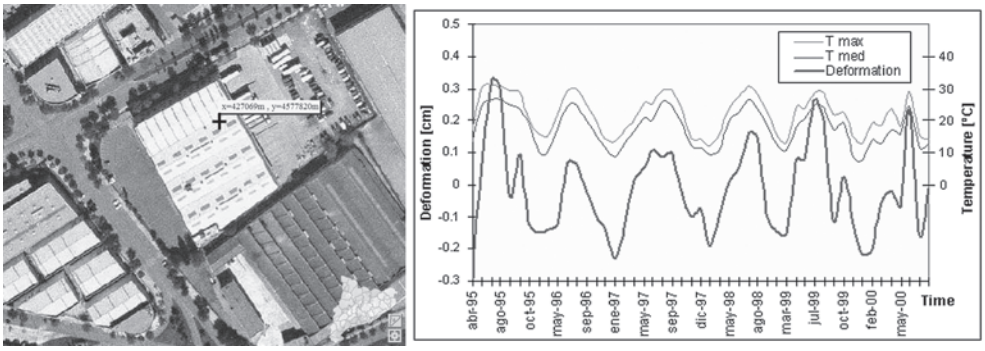

Fig. 3: Estimation of the temporal evolution of deformation of the roof of an industrial building located in the area of Barcelona. Input data: 49 ERS images that cover the period 1995 to 2001. The deformation is probably due to thermal dilation of the portion of the observed roof. Data courtesy of Altamira Information.

ment of algorithms for the exploitation of ERS-Envisat using the SAR permanent scatterers technique", coordinated by Altamira Information (www.altamira-information.com), one of the few commercial companies worldwide that has A-DInSAR capabilities. This result was validated at the Institute of Geomatics. In this case 49, ERS-1 and ERS-2 images were used, which cover the period 1995 to 2001. One may appreciate the highly non-linear behaviour of deformation. The deformation pattern shows a high correlation coefficient (0.84) with the time series of temperatures of Barcelona in the acquisition days of the 49 images. This indicates that the deformation is probably due to thermal dilation of the portion of the observed roof. It is worth noting the magnitude of the deformation oscillation, which ranges in the interval ± 3 mm: this result is useful to get an idea of the sensitivity of the A-DInSAR outcomes.

2) The residual topographic error e_{Topo} represents another interesting type of parameter that can be estimated by the A-DInSAR techniques. e_{Topo} is given by the difference between the true height of the scattering phase centre of a given pixel, and the height given by the employed DEM or digital terrain model (DTM). The information on this parameter is contained in the component $\Phi_{\mathrm{Res\_}Topo}$, which depends linearly on the residual topographic error (Ferretti et al. 2000) with a magnitude, on a given interferogram, which is modulated by its perpendicular baseline $B_{\perp}$. Therefore, given a set of interferograms, the wider is the spectrum of $B_{\perp}$, the better is the configuration to estimate e_{Topo}. This parameter plays an important role only for two specific goals: for A-DInSAR modelling purposes, and for geocoding purposes. As said above, $\Phi_{\mathrm{Res\_}Topo}$ can be explicitly modelled, i. e. can be explained by estimating one parameter e_{Topo} per each pixel. If this parameter is disregarded, $\Phi_{\mathrm{Res\_}Topo}$ will contribute to the non modelled part of $\Delta\Phi_{Int}$, i. e. it will partially affect the estimation of other parameters of interest. Therefore, the estimation of e_{Topo} results in a net benefit for modelling. The second important use of e_{Topo} is the implementation of advanced geocoding procedures for the A-DInSAR products. The standard methods simply employ the same DEM or DTM used in the simulation of Φ_{Topo_Sim} to geocode the DInSAR products. That is, they use an (often rough) approximate value of the true height of the scattering phase centre of a given pixel, which results in a location error in the geocoding. By using the estimated e_{Topo} this kind of error can be largely reduced, thus achieving a more precise geocoding: this may considerably help the interpreta-

Fig. 4: Advanced geocoding of A-DInSAR results over the San Paolo Stadium of Naples (Italy). Pixel location without (left) and with (right) the correction based on the residual topographic error. An optical image of the area is on the background. This result was achieved by using an A-DInSAR technique described in LANARI et al., (2004), with 55 ERS images. (Images courtesy of Dr. RICCARDO LANARI from IRECE-CNR, Naples, Italy).

tion and the exploitation of the A-DInSAR results. An example of advanced geocoding is shown in Fig. 4. It concerns the area of the Stadium of Naples (Italy). The left image shows the location of the measured DInSAR pixels achieved with a standard DEM-based geocoding, while the right image shows a precise location, which was computed by using e_{Topo}, see for details LANARI et al. (2004).

The formal precision that can be achieved in the estimation of e_{Topo} is a function of the distribution of the $B_{\perp}$. Using large baselines, which range in the interval $\pm$ 1200 m, COLESANTI et al. (2003a) achieve a standard deviation of the estimated e_{Topo} that is less than 1 m. Despite the importance of the above uses of e_{Topo}, it is important to note that this parameter describes a rather specific feature, i. e. the height of the radar scattering phase centre, which depends on several factors that drive the dominant mechanism of scattering, e. g. orientation, size, shape, density and dielectric constant. This means that e_{Topo} cannot in general be used to improve the quality of the DEM used in the A-DInSAR procedure. It can only be used to derive a kind of improved ''radar DEM''. Furthermore, it is worth noting that e_{Topo} is only estimated over the ''good pixels'' exploited by the A-DInSAR procedures.

3) The A-DInSAR techniques can estimate the atmospheric phase contribution of each image of the used SAR stack (this contribution is sometimes called Atmospheric Phase Screen, APS), starting from the phase component Φ_{Atm} of the interferograms. Even if this information is usually useless for other applications, it is fundamental to achieve an accurate DInSAR modelling and thus to properly estimate the deformation contribution. In fact, only if APS contributions are properly estimated and removed it is possible to avoid the strong degradation of the DInSAR quality caused by the atmospheric effects. The A-DInSAR strategies used to estimate the APS contributions usually exploit the spatio-temporal correlation characteristics of the APSs, i. e. that the atmospheric effects are usually uncorrelated in time, while they are spatially smooth, e. g. see FERRETTI et al. (2000).

4 Pixel selection: coherence vs. persistent scatterers

Even if SAR sensors perform a regular 2D sampling of the terrain, only the pixels characterized by a low level of Φ_{Noise} are exploited to derive the deformation estimations. This requires adopting a pixel selection criterion. As mentioned above, the loss of coherence results in a noisy interferometric phase. During the interferometric process it is possible to estimate, for each interferogram, the coherence (i. e. the correlation) of the two images that form the given interferogram. The standard DInSAR techniques use this information for the pixel selection, i. e. they perform a coherence-based pixel selection. Note that the same criterion is used by some A-DInSAR techniques (Lanari et al. 2004, Crosetto et al. 2005). Another important class of A-DInSAR techniques use as a pixel selection criterion the stability of the SAR amplitude (Ferretti et al. 2000). The points selected with such a criterion are usually referred to as Permanent or Persistent Scatterers (PS).

The choice of the selection criterion depends on the application at hand. The coherence-based A-DInSAR methods work well over long-term coherent areas: urban, suburban and industrial areas. Their major limitation is that most spaceborne sensors are operated in C-band, see Tab. 2, a frequency in which decorrelation effects are strong in particular over vegetated areas. Furthermore, the repeat cycles of these satellites are rather long: this causes a loss in coherence, and usually prevents the generation of deformation results outside the urban areas. Fig. 5 shows a result derived with a coherence-based A-DInSAR technique. The deformation velocity field is superposed to a SAR amplitude image of the same area. In this case 13 ERS images have been used. In this case different unknown subsidence phenomena have been discovered: this example shows the potential of DInSAR as an "early detection tool" of deformations. Fig. 6 shows a zoom of Fig. 5 over an industrial area. In this second image the geocoded deformation velocities are superposed to an orthoimage. One may notice in Figs. 5 and

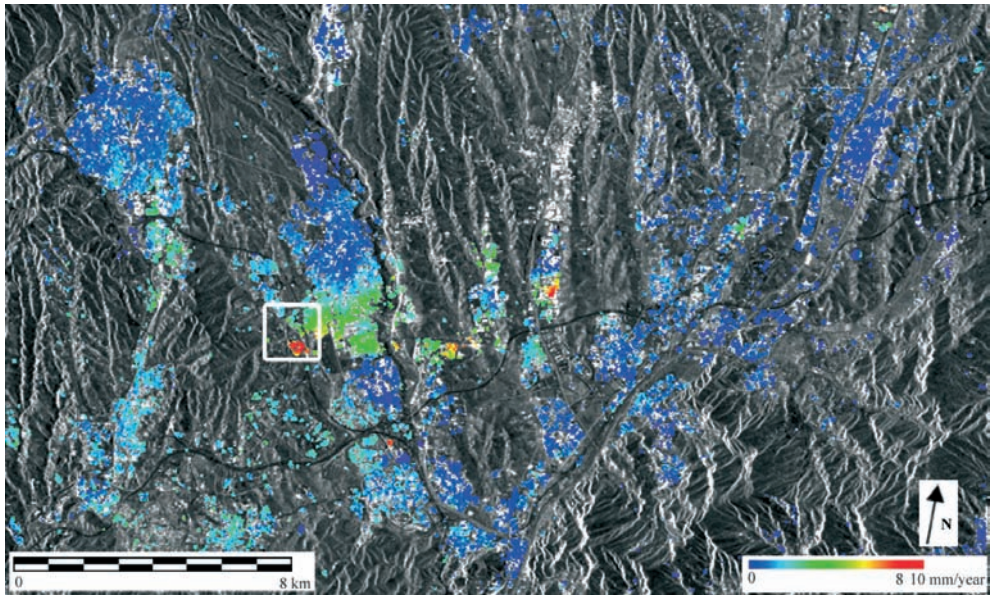

Fig. 5: Coherence-based A-DInSAR analysis over an area of 28 km × 12 km, using 13 ERS images: vertical deformation velocity in the period June 1995 and August 2000. The velocity, in colour, is superposed to a SAR amplitude image of the same area. The areas in grey values are those where no velocity estimation is possible due to coherence loss.

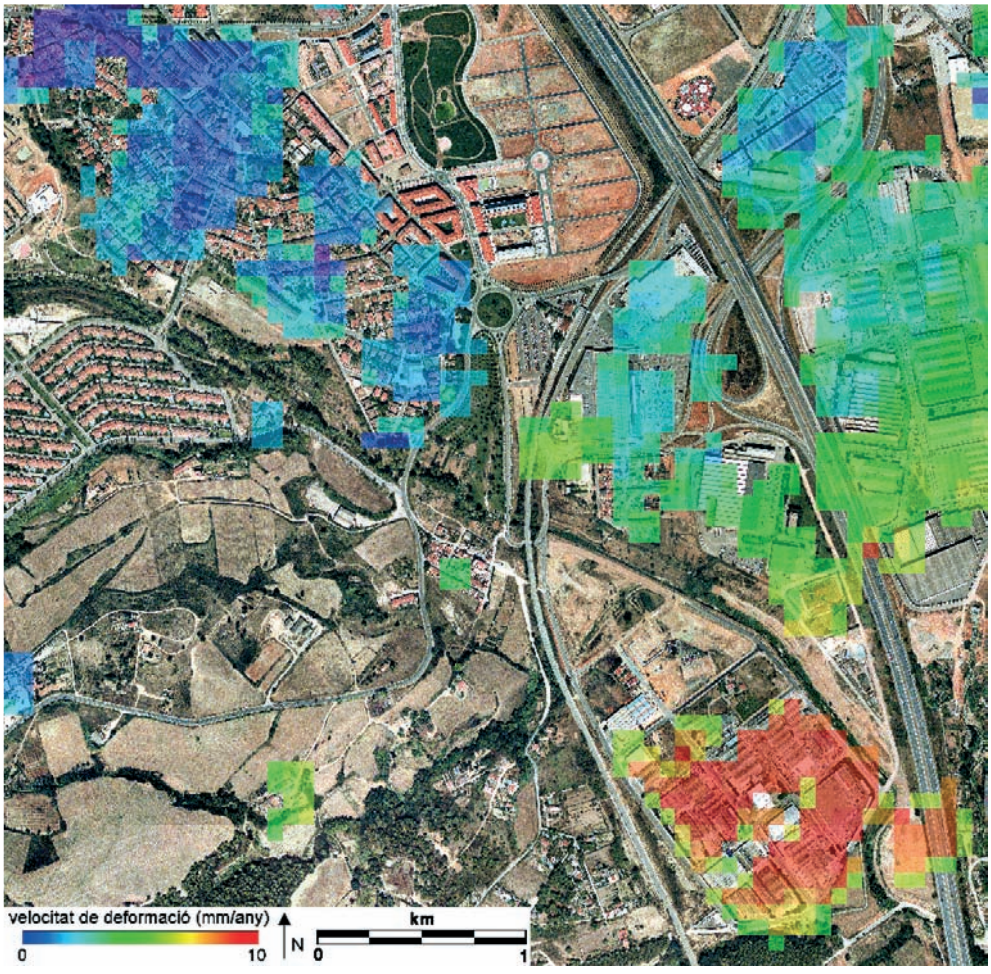

Fig. 6: A-DInSAR analysis over an industrial area, whose location is shown by a white frame in Fig. 5. The vertical deformation velocity field is superposed to a 1:5000 orthoimage of the Cartographic Institute of Catalonia.

6 that over a large part of the analyzed area the deformation cannot be measured, due to a lack of coherence. This result could be probably improved by using PS-based techniques, whose main advantage is to potentially exploit all the coherent targets of the covered scene, even those that are isolated. In fact, the coherence of a given pixel is estimated over a window centred on the same pixel: if a single and very coherent target (e. g. a small man-made object) is located in a very noisy area (e. g. a grass field) it will probably have a low coherence value. This does not occur with the PS techniques, which work at full resolution and which select the pixels without considering the neighbourhood pixels.

5 Available softwares

The importance that DInSAR is gaining as a deformation monitoring tool is reflected in the number of available softwares with DInSAR analysis capabilities. Some of them are listed in Tab. 1. Note that this list is not exhaustive and, more importantly,

Tab. 1: Available software with standard DInSAR or advanced DInSAR capabilities.

Software name	Company/ University	Web site/ type of licence	Platform and software characteristic	DInSAR capabilities
Doris	TU Delft	enterprise.lr.tudelft.nl/doris free license for non-commercial purposes	Unix/Linux/ WinXP (C++ source code available)	Standard DInSAR with ERS1/2, RADARSAT, ENVISAT, JERS. Additional programs for unwrapping (Snaphu) and orbit processing (Getorb) available
Roi_pac	Berkley University	www.openchannelfoundation.org free license for non-commercial purposes	Unix/Linux (C and F90 source code available)	Standard DInSAR with ERS1/2, JERS
Diapason	Developed by CNES	www.altamira-information.com commercial licence distributed by Altamira Information	Linux/Win 95, 98, NT, 2000	Standard DInSAR with ERS1/2, JERS-1, RADARSAT, ENVISAT
Envi	Research Systems Inc. (RSI)	www.rsinc.com/ envi commercial licence	Unix/Linux/ Win2000 and WinXP	Module of ENVI, SARscape, standard DInSAR with ERS1/2, JERS-1, RADARSAT, ENVISAT
Vexcel 3DSAR	Vexcel Corp.	www.vexcel.com commercial licence	Unix/Linux/Windows	Module of the EV-InSAR, CTM – Coherent Target Monitoring, with advanced DInSAR capabilities with ERS1/2, JERS-1, RADARSAT, ENVISAT
Gamma	Gamma	www.gamma-rs.ch/ commercial licence	UNIX, Linux, Win Modular packages in C code available	Advanced DInSAR with ERS1/2, JERS-1, SIR-C, X-SAR, RADARSAT, ENVISAT

that the reported information comes from publicly available documentation: these softwares have not been tested by the authors. The table does not include the software tools developed by research centres that are not commercialized or freely distributed for non-commercial purposes. Moreover, it does not include the tools developed by those private companies that do not commercialise their software. This, for instance, is the case of TRE, based in Milan, and Altamira Information, located in Barcelona.

The first two softwares listed in Tab. 1 are freely available for non-commercial purposes: DORIS, see a description in Kampes et al. (2003), and ROI—PAC. Both of them have the source code available. The DIAPASON is a command line software developed by a research group at the French CNES, which is suitable for advanced users. Some remote sensing software tools include specific modules for standard DInSAR analysis, i. e. the analysis based on single interferograms. This is the case of ENVI, while other packages e. g. ERDAS, seem to provide only tools for InSAR analysis. Example of A-DInSAR commercial tools are those sold by Vexcel and Gamma. This last company, which is based in Switzerland, besides selling its products, provides A-DInSAR analysis services.

6 Data availability

The availability of data acquired by spaceborne sensors represents a key issue for the successful use of DInSAR and especially A-DInSAR techniques that require large series of SAR images. Furthermore, for these techniques plays a fundamental role the image acquisition continuity over large time periods of the same sensor, or compatible sensors, e. g. ERS-1 and ERS-2. The continuity is needed in particular for all the applications characterized by small deformation rates, for those that require long-term deformation monitoring, and in general for the acceptation of the A-DInSAR techniques as operational land deformation monitoring tools. In Tab. 2 the principal SAR missions and satellites that have demonstrated DInSAR capabilities are reported. For each satellite are given at least two references to studies realized with its data. Besides the Seasat mission, which gave the data used to derive the first DInSAR results (Gabriel et al. 1989) but which however had a very short life, the satellite which has provided the data to fully demonstrate the DInSAR potentiality was ERS-1. This satellite has been operative for 10 years, and, more importantly, with its exact copy, ERS-2, has provided a valuable historical archive of interferometric SAR data, which has global spatial coverage and covers a time period of almost 14 years, with the first images that date back to summer 1991. Besides the four references given in the table, there are hundreds of high level scientific publications that demonstrate the success of the ERS mission.

The satellites that are currently operational are RADARSAT-1 and ENVISAT. Various space agencies are planning new missions for earth observation with microwave SAR sensors, e. g. RADARSAT-2 a mission of the Canadian Space Agency in cooperation with other partners; TERRASAR-X of the German Aerospace Centre; COSMO-SKYMED (Constellation of Small Satellites for Mediterranean basin observation) of the Italian Space Agency; and MAPSAR, a joint Brazilian-German project which is expected to have high spatial resolution L-band capabilities for polarimetry, and interferometry, see Schroeder et al. (2005). A special mention is reserved by the continuity issue between the ERS and Envisat missions of the European Space Agency. It would be very useful to guarantee in the near future the continu-

Tab. 2: Main SAR missions with interferometric SAR capabilities.

Satellite	Frequency [GHz]	Start mission	End mission	Wavelength [cm]	DInSAR works based on these data
SEASAT	1.275	1978	1978	23.5	Gabriel, A. K et al. (1989), Li and Goldstein (1990)
ERS-1	5.300	1991	2000	5.6	Massonnet D. et al. (1993), Goldstein et al. (1993)
ERS-2	5.300	1995	–	5.6	Ferretti A. et al. (2000), Rosen P.A. et al. (2000)
JERS-1	1.275	1992	1998	23.5	Kimura and Yamaguchi (2000), Fujiwara et al. (1998)
RADARSAT-1	5.300	1995	–	5.6	Wegmüller et al. (2000a), Lu et al. (2003)
ENVISAT	5.331	2002	–	5.6	Wegmüller et al. (2000b), Arnaud et al. (2003)
RADARSAT-2	5.300	*2006*	–	5.6	–

ity of the existing 14 year archive of interferometric SAR images. There is a temporal overlap between the ERS-2 and Envisat missions: this new instrument could in principle continue the success of the ERS satellites and increase the value of the archived ERS data. In reality, there is a big problem in mixing Envisat and ERS data: the two systems have slightly different radar frequencies, and this prevents the simple combination of their data (the interferometric phase is strongly dependent on the wavelength, and thus on the radar frequency).

In the last two years a big effort has been devoted to this topic, e. g. see ARNAUD et al. (2003) which describe the generation of the first ERS-Envisat cross-interferogram. Without going into details, it is worth mentioning that combining ERS and Envisat data for A-DInSAR applications, i. e. using mixed image stacks of ERS and Envisat, under given conditions is possible, see some interesting results in DURO et al. (2005). In particular, this is possible by taking advantage of a special feature of the PS: they usually are much smaller than the resolution cell, and thus have a reduced geometric decorrelation due to the fact that the two SAR images are not acquired exactly from the same point.

7 DInSAR quality and validation issues

An important goal of the current A-DInSAR research is to provide deformation observations characterized by high quality standards (accuracy, precision and reliability), which are comparable with those of the observations coming from the geodetic techniques. As mentioned in previous sections, the above goal can only be achieved using a high observation redundancy (i. e. by using several SAR images of the same area), and by implementing appropriate data analysis tools. In the last few years there has been an increasing attention to the A-DInSAR estimation quality, e. g. see COLESANTI et al. (2003a), which provide a comprehensive error budget analysis of the Permanent Scatterers technique. Another topic that is receiving particular attention is the validation of the A-DInSAR results, e. g. see DURO et al. (2005). In general, the validation is difficult, especially for the extension of the measured areas: often there are no reference data are available. An additional complication comes from the relatively high quality of the A-DInSAR and the consequent difficulty to get suitable reference data of higher quality.

8 Conclusions

In this paper the state-of-the-art of DInSAR techniques for land deformation monitoring has been analysed, discussing in particular:

- the main differences between the standard DInSAR techniques, which are based on a single SAR image pair, and the advanced DInSAR techniques, which exploit large sets of images acquired over the same area,
- the importance of the criteria used to select the pixels suitable to deformation measurement,
- the availability of DInSAR software tools, and of data coming from spaceborne SAR sensors,
- and finally some aspects related to the quality and validation of the DInSAR results.

Different other important topics are not considered in this paper, e. g. an analysis of the limitation of the techniques, the discussion of key technical aspects, such as the phase unwrapping, and the possible synergy with data coming from other sources, etc. This aspects are treated in detail in more comprehensive DInSAR reviews, see ROSEN et al. (2000), BAMLER & HARTL (1998), and HANSSEN (2001).

Acknowledgements

This work has been partially supported by the Spanish Ministry of Science and Technology, through the research project REN2003-00742, AURORAE. The authors acknowledge ALAIN ARNAUD and JAVIER DURO from Altamira Information for pro-

viding their A-DInSAR results over the city of Barcelona, and Riccardo Lanari from IRECE-CNR, Naples, for providing the advanced geocoding results over the San Paolo Stadium of Naples.

References

Amelung, F., Galloway, D.L., Bell, J.W. et al., 1999: Sensing the ups and downs of Las Vegas: InSAR reveals structural control of land subsidence and aquifer-system deformation. – Geology **27**(6): 483–486.

Amelung, F., Jonson, S., Zebker, H.A. & Segall, P., 2000: Widespread uplift and 'trapdoor' faulting on Galápagos volcanoes observed with radar interferometry. – Nature **407:** 993–996.

Arnaud, A., Adam, N., Hanssen, R. et al., 2003: ASAR ERS interferometric phase continuity. – IGARSS, 21–25 July 2003, Toulouse (France), (CDROM).

Bamler, R. & Hartl, P., 1998: Synthetic aperture radar interferometry. – Inverse Probl. **14:** R1–R54.

Colesanti, C., Ferretti, A., Novali et al., 2003a: SAR monitoring of progressive and seasonal ground deformation using the Permanent Scatterers Technique. – IEEE T Geosci. Remote **41**(7): 1685–1701.

Colesanti, C., Ferretti, A., Prati, C. & Rocca, F., 2003b: Monitoring landslides and tectonic motions with the Permanent Scatterers Technique. – Eng. Geol. **68:** 3–14.

Crosetto, M., Castillo, M. & Arbiol, R., 2003: Urban subsidence monitoring using radar interferometry: Algorithms and validation. – Photogr. Eng. Rem. S. **69**(7): 775–783.

Crosetto, M., Crippa, B. & Biescas, E., 2005: Early detection and in-depth analysis of deformation phenomena by radar interferometry. – Eng. Geol. **79** (1-2): 81–91.

Duro, J., Closa, J., Biescas, E. et al., 2005: High Resolution Differential Interferometry using time series of ERS and ENVISAT SAR data. – Proc. of the 6th. Geomatic Week, February 2005, Barcelona, Spain (CDROM).

Ferretti, A., Prati, C. & Rocca, F., 2000: Nonlinear subsidence rate estimation using permanent scatterers in differential SAR interferometry. – IEEE T Geosci. Remote **38**(5): 2202–2212.

Ferretti, A., Prati, C. & Rocca, F., 2001: Permanent scatterers in SAR interferometry. – IEEE T Geosci. Remote **39** (1): 8–20.

Fujiwara, S., Rosen, P., Tobita, M. & Murakami, M., 1998: Crustal deformation measurements using repeat-pass JERS-1 synthetic aperture radar interferometry near Izu Peninsula. – Japan. J. Geophys. Res. **103:** 2411–2424.

Gabriel, A.K., Goldstein, R.M. & Zebker, H.A., 1989: Mapping small elevation changes over large areas: differential radar interferometry. – J. Geophys. Res. **94** (B7): 9183–9191.

Gatelli, F., Monti Guarnieri, A., Parizzi, F., et al., 1994: The Wavenumber Shift in SAR Interferometry. – IEEE T Geosci. Remote **32**(4): 855–865.

Goldstein, R.M., Englehardt, H., Kamb, B. & Frolich, R.M., 1993: Satellite radar interferometry for monitoring ice sheet motion: application to an Antarctic ice stream. – Science **262:** 1525–1530.

Hanssen, R., 2001: Radar interferometry. – Kluwer Academic Publishers, Dordrecht (The Netherlands).

Hilley, G.E., Bürgmann, R., Ferretti, A. et al., 2004: Dynamics of Slow-Moving Landslides from Permanent Scatterer Analysis. – Science **304:** 1952–1955.

Kampes, B.M., Hanssen, R.F. & Perski, Z., 2003: Radar Interferometry with public Domain Tools. – Proc. of Fringe 2003, SP-550, ESA (CD-ROM).

Kimura, H. & Yamaguchi, Y., 2000: Detection of landslide areas using satellite radar interferometry. – Photogramm. Eng. Rem. S. **66**(3): 337–344.

Kwok, R. & Fahnestock, M.A., 1996: Ice sheet motion and topography from radar interferometry. – IEEE T Geosci. Remote **34**(1): 189–200.

Lanari, R., Mora, O., Manunta, et al., 2004: A small-baseline approach for investigating deformations on full-resolution differential SAR interferograms. – IEEE T Geosci. Remote **42** (7): 1377–1386.

Li, F. & Goldstein, R.M., 1990: Studies of multibaseline spaceborne interferometric synthetic aperture radars. IEEE T Geosci. Remote **28**(1): 88–97.

Lu, Z., Wright, T. & Wicks, C., 2003: Deformation of the 2002 Denali Fault Earthquakes, Mapped by Radarsat-1 Interferometry. – EOS **84**(41):. 430–431.

Massonnet, D., Rossi, M., Carmona, C. et al., 1993: The displacement field of the Landers earthquake mapped by radar interferometry. – Nature **364:** 138–142.

Massonnet, D. & Feigl, K. L., 1998: Radar interferometry and its application to changes in the earth's surface. – Reviews of Geophysics **36** (4): 441–500.

Massonnet, D. & Sigmundsson, F., 2000: Remote sensing of volcano deformation by radar interferometry from various satellites. – In: Mouginis-Mark et al. (eds.): Remote sensing of active volcanism. – Geophysical Monographs 116, American Geophysical Union, pp. 207–221.

Peltzer, G., Rosen, P., Rogez, F. & Hudnut, K, 1996: Postseismic rebound in fault stepovers caused by pore fluid flow. – Science **273:** 1202–1204.

Rosen, P., Werner, C., Fielding, E. et al., 1998: Aseismic creep along the San Andreas fault northwest of Parkfield, CA measured by radar interferometry. – Geophys. Res. Lett. **25**(6): 825–828.

Rosen, P.A., Hensley, S., Joughin et al., 2000: Synthetic Aperture Radar Interferometry. – Proc. of the IEEE **88**(3): 333–382.

Schroeder, R., Puls, J., Hajnsek, I. et al., 2005: MAPSAR: a small L-band SAR mission for land observation. – Acta Astronautica **56**(1-2): 35–43.

Wegmuller, U., Strozzi, T. & Tosi, L., 2000a: Differential SAR interferometry for land subsidence monitoring: methodology and examples. – Proc. SISOLS 2000, 25–29 September 2000, Ravenna (Italy).

Wegmüller, U., Strozzi, T. & Tosi, L., 2000b: ERS and ENVISAT differential SAR interferometry for subsidence monitoring. – Proc. ERS-ENVISAT Symposium, 16–20 October 2000, Gothenburg (Sweden).

Zebker, H.A., Rosen, P.A., Goldstein, R.M. et al., 1994: On the derivation of coseismic displacement fields using differential radar interferometry: The Landers Earthquake. – J. Geophys. Res. **99** (B10): 19617–19634.

Addresses of the authors:

Dr. Michele Crosetto
e-mail: michele.crosetto@ideg.es
Ms. Erlinda Biescas
e-mail: erlinda.biescas@ideg.es
Mr. Oriol Monserrat
e-mail: oriol.monserrat@ideg.es
Ms. Marta Agudo
e-mail: marta.agudo@ideg.es
Institute of Geomatics, Parc Mediterrani de la Tecnologia, Av. del Canal Olímpic, s/n, Castelldefels (Barcelona), E-08860, Spain
Tel.: +34-93-5569294, Fax: +34-93-5569292

Prof. Dr. Bruno Crippa
e-mail: bruno.crippa@unimi.it
Department of Earth Sciences, University of Milan, Via Cicognara 7, I-20129 Milan, Italy
Tel: +39-02-50318474, Fax: +39-02-50318489

Ms. Paz Fernández
e-mail: pazferol@ugr.es
Departamento de Ingeniería Civil, Universidad de Granada, ESCCP, Edificio Politécnico, Campus de Fuentenueva s/n, E-18071, Granada, Spain
Tel: +34-958-240486, Fax: +34-958-246138

Manuskript eingereicht: Juni 2005
Angenommen: Juli 2005